8888–8898 *Nucleic Acids Research, 2019, Vol. 47, No. 16* *Published online 2 August 2019*
doi: 10.1093/nar/gkz649

Sharp kinking of a coiled-coil in MutS allows DNA binding and release

Doreth Bhairosing-Kok†, Flora S. Groothuizen†, Alexander Fish†, Shreya Dharadhar, Herrie H.K. Winterwerp and Titia K. Sixma*

Division of Biochemistry and Oncode Institute, Netherlands Cancer Institute, 1066 CX Amsterdam, the Netherlands

Received November 17, 2018; Revised July 11, 2019; Editorial Decision July 12, 2019; Accepted July 15, 2019

ABSTRACT

DNA mismatch repair (MMR) corrects mismatches, small insertions and deletions in DNA during DNA replication. While scanning for mismatches, dimers of MutS embrace the DNA helix with their lever and clamp domains. Previous studies indicated generic flexibility of the lever and clamp domains of MutS prior to DNA binding, but whether this was important for MutS function was unknown. Here, we present a novel crystal structure of DNA-free *Escherichia coli* MutS. In this apo-structure, the clamp domains are repositioned due to kinking at specific sites in the coiled-coil region in the lever domains, suggesting a defined hinge point. We made mutations at the coiled-coil hinge point. The mutants made to disrupt the helical fold at the kink site diminish DNA binding, whereas those made to increase stability of coiled-coil result in stronger DNA binding. These data suggest that the site-specific kinking of the coiled-coil in the lever domain is important for loading of this ABC-ATPase on DNA.

INTRODUCTION

The DNA mismatch repair (MMR) pathway is responsible for maintaining genetic information by correcting base-substitution and insertion-deletion mismatches, generated during DNA replication (1,2). MMR deficiency results in a mutator phenotype and in humans it can predispose to cancer, referred to as HNPCC or Lynch syndrome (3). MutS initiates the repair by scanning the DNA for mismatches. Upon mismatch detection, it signals for repair by forming a sliding clamp that activates MutL (4,5). MutL then activates the downstream repair, which includes nicking the newly replicated strand, unwinding the DNA and resynthesis of the daughter strand.

MutS proteins belong to the ATP-binding cassette (ABC) ATPases and are evolutionarily conserved from bacteria to mammals. MutS forms constitutive dimers, while some prokaryotic MutS homologs can also tetramerize through their C-terminal domain, but this is not required for MMR (6–8). In eukaryotic cells, the MutS homologs that are active in MMR form heterodimers (MSH2/MSH6 or MSH2/MSH3) (9). In both prokaryotes and eukaryotes, MutS acts as a heterodimer during MMR. During mismatch binding, both monomers embrace the DNA helix with their lever and clamp domains (10–13) but only one of the monomers recognizes the DNA mismatch through its mismatch-binding domain.

The binding of the MutS clamp domains around the DNA helix is expected to be a general feature, regardless of the presence of a mismatch. The crystal structure of DNA-free *Thermus aquaticus* MutS indicated disorder of large portions of MutS in the absence of DNA. The clamp, lever and mismatch domains were not ordered while the dimer itself was kept intact (11). Conformational freedom of the clamp domains was also observed in SAXS studies with the DNA-free protein (8). Both studies indicate that in the absence of DNA, the clamp and lever domains of MutS dimers are flexible, but how such flexibility is achieved was unclear. The lever domains of MutS are composed of two α-helices, forming a left-handed antiparallel coiled-coil (14). Other ABC-ATPase family members, such as Rad50 and the Structural Maintenance of Chromosomes (SMC) family have coiled-coil levers that are even more extended. The latter proteins were shown to have conformational flexibility in their coiled-coils in atomic force microscopy (AFM) and rotary shadowing electron microscopy (EM) analyses (15–18).

Here we present a novel crystal structure of a DNA-free *Escherichia coli* MutS dimer, where the lever domains display an unexpected kink, resulting in a displacement of the clamp domains relative to the mismatch-bound state (10). In our structure, the conformational freedom originates from hinging of specific regions in the lever domains. We wondered if the ability to kink rather than generic flexibility could be important for MutS function. We studied the effect of mutations at the kinking site on different steps in MutS activation, including DNA binding, mismatch recognition, ATP-dependent clamp formation and loading of

*To whom correspondence should be addressed. Tel: +31 20 5121959; Email: t.sixma@nki.nl
†The authors wish it to be known that, in their opinion, the first three authors should be regarded as Joint First Authors.

MutL. The data indicate that the defined hinge is relevant for DNA binding by this ABC-ATPase.

MATERIALS AND METHODS

Proteins

MutS mutants were created in the *mutS* gene in vector pET-3d and LOCK1, a MutS double cysteine variant E435C R449C, was created in a *mutS* cysteine free vector (19,20), using the QuikChange Site-Directed Mutagenesis Kit (Stratagene) and appropriate primers (IDT). All MutS and MutL proteins were expressed and purified as described (21), except for mutants MutS FLEX2 and MutS FLEX3 where the lysis buffer contained 10% glycerol and an increased salt concentration of 400 mM.

Crystallography

Crystallization of full-length DNA-free MutS P839E was performed using 50 μM MutS (in 25 mM Hepes 7.5, 150 mM NaCl, 10 mM $MgCl_2$) mixed with ADP (final concentration 50 μM) in 200 nl. The protein was crystallized using vapor diffusion with 3–8% dioxane, 1.4–1.7 mM $(NH_4)_2SO_4$ and 100 mM Hepes pH 7.0. The crystal was transferred to mother liquor supplemented with 30% glycerol before flash cooling it in liquid nitrogen.

Crystallographic data were collected at ESRF beamline ID14-4 and was processed using iMosflm (22) and Scala (23). The initial structure was solved using molecular replacement for the ATPase domain in Phaser (24) with part of chain A of PDB entry 1WB9 as search model and stepwise addition of domains. Structure refinement was performed using Buster (25), Refmac5 (26) and PDB-REDO (27). Residues 12–80 (mismatch binding domain) in chain A and residues 442–503 (clamp domain) in chain B have density that is not very well defined, indicating some flexibility within the crystal. They were placed in the structure as rigid bodies, using the conserved fold of the mismatch binding domain and clamp domain, respectively. See Table 1 for crystallographic statistics.

Protein stability measurements

Protein stability was assayed using a Prometheus NT.48 (Nanotemper). WT or mutant MutS proteins were diluted to 1 mg/ml and subjected to a temperature gradient to determine melting temperatures (T_m), which were read out by changes in tryptophan fluorescence. Analytical gel filtration was performed for MutS WT and all mutants on a S200 5/100 (GE Healthcare) in 25 mM Hepes 7.5, 250 mM KCl and 1 mM DTT on an Akta Micro system.

Equilibrium DNA binding

Fluorescence polarization measurements to assess DNA-binding affinities of WT and mutant MutS proteins were performed in buffer consisting of 25 mM Hepes pH 7.5, 150 mM KCl, 5 mM $MgCl_2$, 0.05% Tween-20. A concentration of 0.5 nM of 5′ labeled TAMRA-21-bp DNA with a mismatch at position 9 (5′-TAMRA-AGCTGCCAGGC ACCAGTGTCA annealed with TGACACTGGTGCTTG GCAGCT) was used as fluorescent probe. MutS proteins were serially diluted in black flat-bottomed 384-well plates (Corning) in 30 μl volumes. The plate was equilibrated at RT for 5 min, after which polarization of the TAMRA label was read out in a PHERAstar FS machine (BMG Labtech) with a 540/590 (excitation/emission) FP module. K_d^{app} values were determined using GraphPad Prism 7.02.

Table 1. Crystallographic data and refinement statistics

Data collection	
λ (Å)	0.934
Resolution range (Å)[a]	80.2–2.6 (2.67–2.6)
Completeness (%)	98.1 (94.2)
I/σ(I)	4.6 (1.4)
R_{merge} (%)	0.30 (1.2)
Space group	P 2_1 2_1 2_1
Cell dimensions (Å)	113.38 113.53 158.90
Total no. of observations	253695 (17401)
Total no. of unique reflections	62205 (4381)
Multiplicity	4.1 (4.0)
Wilson's *B*-factor (Å^2)	32.2
Refinement	
No. of atoms (protein/solvent)	12198/254
Average *B*-factor (Å^2)	59
R_{free} reflections	3051 (4.91%)
R_{work}/R_{free} (%)	20.6/25.7
Ramachandran[b]	1450/73/0
Bond r.m.s.z/r.m.s.d. (Å)	0.53/0.0106
Angle r.m.s.z/r.m.s.d.(°)	0.78/1.27

[a]Numbers within parentheses refer to the highest resolution shell.
[b]Number of residuals favored/allowed/outliers.

Surface plasmon resonance analysis of DNA-binding kinetics

Kinetics of MutS binding to 21-bp DNA containing a GT mismatch (sequence, see above), which was attached to a streptavidin chip via a biotin-conjugated $(dT)_{20}$ linker, was determined using surface plasmon resonance (SPR). The measurements were performed in a Biacore T200 system (GE Healthcare) at 25°C with the same setup as described previously (8,21). Data analysis of FP and SPR experiments was done using GraphPad Prism 7.02 (GraphPad Software Inc.). In order to calculate apparent equilibrium binding constants (K_d^{app}) binding responses were plotted as function of protein concentration and fitted with one site binding equation:

$$Y = \frac{B\max \times X}{K\mathrm{d} + X} + \text{Background}$$

Where Y = binding response; X = protein concentration; Background = background response, B_{max} = Maximum binding response; K_d = apparent equilibrium binding constants.

In order to calculate apparent dissociation rate constants (k_{off}^{app}) the dissociation phases of the SPR sensograms were fitted with one phase decay equation:

$$Y = (Y_0 - \text{Plateau}) * e^{-k\times(t-t_0)} + \text{Plateau}$$

Where Y = binding response; Y_0 = initial binding response; Plateau = final plateau after dissociation; $k = k_{off}^{app}$; t_0 = dissociation starting time.

SPR to analyze MutL binding

Binding kinetics of MutS-MutL to 100-bp containing a GT mismatch was performed in the same set-up (8,21), with the addition 1 mg/ml BSA and 1 mM ATP. Biotinylated DNA was immobilized on a streptavidin chip to a signal of ∼15.0 RU. Double biotinylated DNA (both 5′ ends) were used as a blocked end oligo. MutS injections of 1200 nM for 60 s were followed by MutL injections for 120 s with concentrations ranging from 0 to 2048 nM. High concentration for MutS was chosen to achieve a full binding for all MutS mutants. In between individual cycles, SA chips were regenerated with 0.5% SDS. MutL binding analysis involved normalization on MutS binding at 60 s and subtracted for MutS binding, therefore making it possible to fit K_d^{app} for MutL binding using GraphPad Prism 7.

For titration of ATP in this context, the same DNA was immobilized. Experiments were performed using the same buffer but lacking ATP. Again 1200 nM MutS was injected for 60 s, followed by a second injection of 120 s containing buffer (control), 0.5, 4 or 32 μM ATP, or 400 nM MutL supplemented with 0.5, 4 or 32 μM ATP.

Crosslinking of LOCK1

A double cysteine mutant E435C R449C (LOCK1) was reduced at 80 μM with 10 mM DTT for 30 min and dialyzed o/n at 4°C into binding buffer (25 mM Hepes 7.5, 150 mM KCl, 5 mM $MgCl_2$) to remove DTT. Crosslinkers $BM(PEG)_2$ (linker length 14.7 Å) and $BM(PEG)_3$ (linker length 17.8 Å) (Sigma) were dissolved in DMSO to a final concentration of 50 mM. Crosslinker was added in 30-fold molar excess over the MutS-monomer concentration and incubated for 3 h at 4°C. Excess of crosslinker was removed using Zeba spin column (7K MWCO, 2 ml, ThermoFisher) and crosslinked MutS was used for DNA-binding kinetics using SPR. SDS-PAGE gel analysis was used to confirm the absence of MutS inter-crosslink dimers (not shown).

Crosslinked LOCK1 was added to 100-bp containing a GT mismatch (21) in 10:1 ratio ([DNA]:[MutS monomer]), incubated for 30 min at RT and analyzed on an Akta Micro using Superdex 200 5/150 (in binding buffer). Using crosslinked LOCK1 and LOCK1, we could examine the binding affinity of the mixed sample. Both proteins were mixed in a 1:1 ratio and incubated for 30 min at RT to form a new equilibrium of heterodimers and homodimers. After 30 min, dilutions were made for SPR experiments (see details above). For all SPR experiments regarding LOCK1, the binding buffer was supplemented with 1 mg/ml BSA.

RESULTS

Crystal structure of DNA-free MutS

Full-length *E. coli* MutS P839E, which does not tetramerize (8), was crystallized in the absence of DNA and its structure was solved at a resolution of 2.6 Å (Table 1 and Figure 1A). Structure solution required a step-wise approach, as domains were rearranged with respect to each other and to other previously determined structures, preventing straightforward molecular replacement. The structure was solved by first placing the ATPase domains, followed by stepwise addition of other domains. In the final structure, the connector and mismatch binding domains can be positioned, but they are poorly resolved. In contrast to most other structures, the full-length protein was used for crystallization. However, the C-terminal tetramerization domains were not resolved in the density, indicating that their position is not stabilized by crystal contacts in this crystal form. This flexible positioning of the C-terminal domains is in line with SAXS analysis (8).

In this structure, the homodimer of MutS adopts an asymmetric conformation, where domains are arranged differently between the two monomers; this is true for lever, clamp connector and mismatch binding domains. However, the ATPase domains are symmetric, in contrast to mismatch-bound *E. coli* MutS structures. In the presence of excess nucleotides, binding of two ADP nucleotides was the most abundant state in native mass-spectrometry measurements (28). Both monomers bind ADP, but no density can be seen for magnesium. This lack of magnesium was previously observed in other DNA-free structures of MutS homologs (11,29).

Kinking of lever domains MutS

A remarkable feature in this DNA-free crystal structure is the position and orientation of the clamp and lever domains of both monomers (Figure 1). One of the clamp domains has moved toward the core of the dimer (inward kink, 23°), relative to mismatch-bound *E. coli* MutS, whereas the clamp domain in the other subunit moved outward (outward kink, 66°). Strikingly, both motions originate from a sharp kink in the same region; residues 440–443 and residues 515–518 in helix 1 and 2 of the coiled-coil respectively, within the lever domain (Figure 1B).

The two lever domains adopt an orientation and conformation that is changed relative to other MutS structures (8,10,29,30). Interestingly, these parts of the helices showed relatively high *B*-factors in the mismatch-bound MutS structures, already suggesting some degree of disorder (10). The presence of these defined hinge points suggests a way for MutS dimers to 'open up' and allow a DNA helix to enter the DNA-binding site, while DNA could also be released in this manner if no mismatch is found and/or sliding clamp is formed. We therefore hypothesize that this crystal structure represents a conformation of MutS that precedes DNA binding.

Mutations to influence the kinking in the lever domain

We wondered whether the kink-movements in the lever domains were essential for DNA binding. Therefore, we studied the kinking of the lever domains in two ways: (i) by making several mutants in the coiled-coil region that should affect the kinking-ability (Figure 2A and B) and (ii) by locking MutS in a kinked-outward conformation via crosslinking of two cysteines in one of the helices of the coiled-coil (Figure 2C).

We made mutants to affect the coiled-coil stability in the hinge-region of both helices. The lever domains of MutS form a left-handed antiparallel coiled-coil arrangement (14) (Figure 2A). Coiled-coil structures are common structural

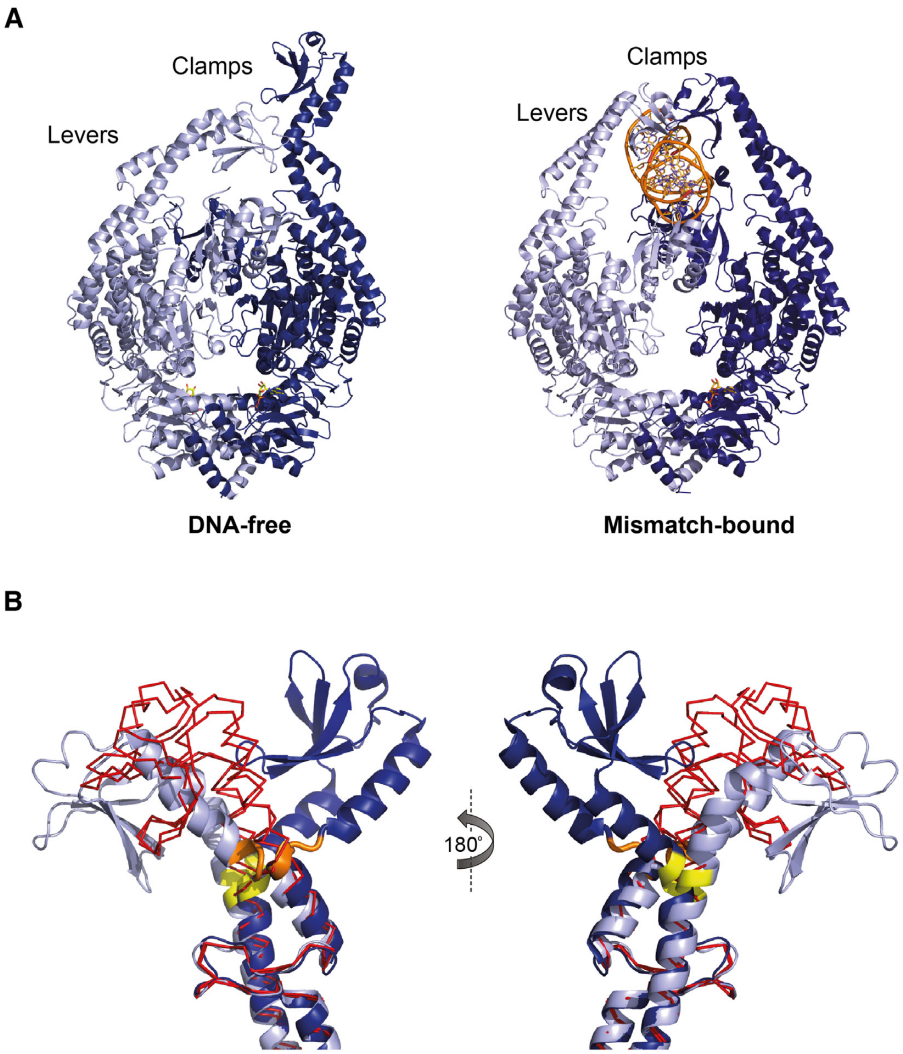

Figure 1. DNA-free crystal structure of MutS with differently positioned clamp domains. (**A**) Cartoons of crystal structure of apo-structure and mismatch-bound (PDB entry: 1E3M) *Escherichia coli* MutS. The two monomers are shown as dark blue and light blue cartoons, and DNA and ADP are shown in orange. (**B**) Superposition to show the kinking that reorients the clamp domains of both monomers in the apo-structure (color as in A) relative to mismatch-bound MutS (shown as red ribbons).

motifs in which helices wrap around each other to form a super helix. While the effect of sequence variation on coiled-coil stability is not fully understood, hydrophobic residues such as leucines and alanines at the *a* and *d* positions of the heptad repeats should facilitate dimer interaction (31). Similarly, charged residues such as glutamate or lysine at the *e* and *g* positions seem to facilitate interhelical electrostatic interactions (31) (Figure 2A). Both helices of the coiled-coil are kinked in the DNA-free structure. Therefore, we hypothesized that if we can create a MutS mutant that has less ability to kink, MutS will be more stable in the closed conformation and will remain a stable complex with DNA. Inversely, the more the kink will be promoted, the less stable the coiled-coil will be and the DNA binding ability will decrease. Using this hypothesis, we designed several mutants aimed to stabilize or perturb the coiled-coil, to investigate the importance of the kinking that we observed in our crystal structure.

We aimed to promote stabilization of the coiled-coils by introducing hydrophobic residues at position *a* and *d*, resulting in MutS mutants STAB1–3 (Figure 2). In addition, STAB4 was made with the additional charged residues at position *e* and *g* to allow more ionic interactions. Conversely we introduced Pro/Gly/Pro motifs at the hinge region, which should destabilize the hinge by weakening the coiled-coil stability and make the hinge more flexible. These MutS mutants were named FLEX1 and FLEX2 and we also generated a combination of these, FLEX3 (Figure 2).

The second approach was to generate a double cysteine mutant of MutS (LOCK1), which should allow locking the MutS dimer in the outward-kinked conformation in both monomers by crosslinking the two sides of the helix using a bismaleimide crosslinker with a suitable length (Figure 2C).

Since mutations affect the secondary structure, they can also influence overall protein stability. Therefore, all mutant proteins were subjected to thermostability measurements

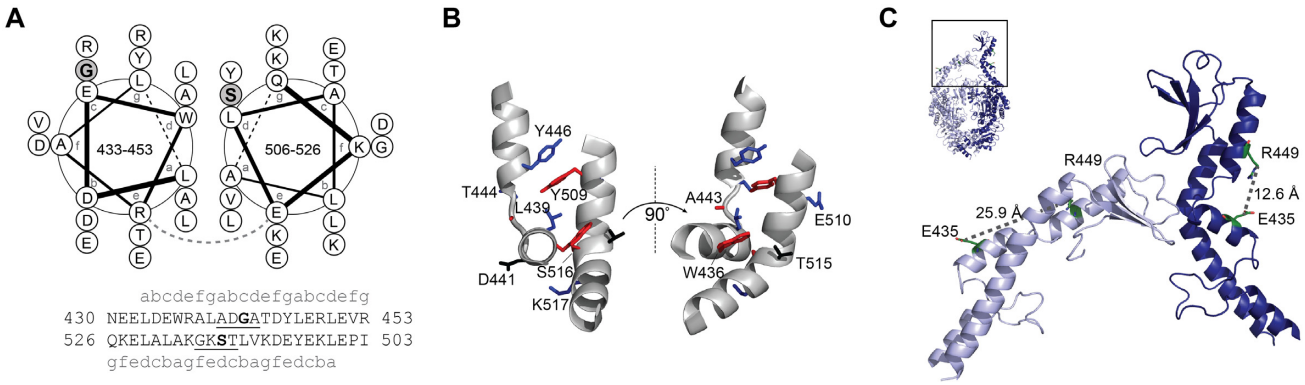

Protein		Mutations	Description
Aimed to promote stable coiled-coil			
STAB1	430 NEELDEWRALAPAVTDYLERLEVR 453 526 QKELALAKGKSTLVKDEFEKLEPI 503	D441P/G442A/A443V Y509F	Promote helical fold in *h1*, increase *cc* packing with A443V/Y509F
STAB2	430 NEELDEWRALADGATDYLERLEVR 453 526 QKELALAKGKATLVKDEYEKLEPI 503	S516A	Promote helical fold at kink in *h2*
STAB3	430 NEELDELRALADGATDYLERLEVR 453 526 QKELALAKGKATLVKDELEKLEPI 503	W436L/Y509L/S516A	Promote quality of hydrophobic core of *cc*
STAB4	430 NEELDELRAEADGAEDELERLEVR 453 526 QKELALAKGKATLVKDKLEKLEPI 503	W436L/L439E/T444E/Y446E Y509L/E510K/S516A	Promote quality of hydrophobic core and salt bridges of *cc*
Aimed to promote locked kink-out conformation			
LOCK1	430 NEELDCWRALADGATDYLECLEVR 453 526 QKELALAKGKSTLVKDEYEKLEPI 503	E435C/R449C	Two cysteines residues for crosslinking
Aimed to promote destabilization coiled coil			
FLEX1	430 NEELDEWRALAPGPTDYLERLEVR 453 526 QKELALAKGKSTLVKDEYEKLEPI 503	D441P/A443P	Pro/Gly/Pro motif in *h1*
FLEX2	430 NEELDEWRALADGATDYLERLEVR 453 526 QKELALAKGPGPLVKDEYEKLEPI 503	T515P/S516G/K517P	Pro/Gly/Pro motif in *h2*
FLEX3	430 NEELDEWRALAPGPTDYLERLEVR 453 526 QKELALAKGPGPLVKDEYEKLEPI 503	D441P/A443P T515P/S516G/K517P	Pro/Gly/Pro motif in *h1* and *h2*

h1 = helix 1 (kinks around residue 442); *h2* = helix2 (kinks around residue 516); *cc* = coiled coil

Figure 2. The coiled-coil in the lever domain of MutS. (**A**) Helical wheel representation of the coiled-coil in the lever domain of WT MutS. Sequences of the helices and their corresponding heptad assignment are written below. The residues around which the kinking takes place are underscored. Table below shows all mutants that were made to study the coiled-coil stability. Positions on helical wheel were chosen first and suitable mutation were made on specific positions. (**B**) Residues mutated on hydrophobic core positions in coiled-coil (*a* and *d*) are shown in red. Residues that could contribute to stability due to ionic interactions (*e* and *g*) are shown in blue. Remaining mutants are colored in black. (**C**) MutS can be locked in a kink-open conformation by creating a double cysteine MutS and creating a bridge between position 435C and 449C using bismaleimide-activated PEG compound. This is unique for the kink-open conformation since the kink-in and mismatch-bound conformation (not shown) will not allow this due to distance and sterical hindrance.

and compared to WT (Table 2). We found that the mutations had only marginal effects on the stability of the protein, as indicated by melting temperature for all variants, with the exception of LOCK1 and FLEX3. In addition, the purification of MutS FLEX2 and FLEX3 required higher salt and glycerol during lysis, indicating lower solubility, but this was not observed for the LOCK1 mutant. Results on these three mutants must therefore be interpreted with caution. In addition, analytical gel filtration profiles of all variants show similar elution profiles, indicating that no major conformational changes have occurred (Supplementary Figure S1)

Table 2. Properties of the MutS variants used in this study

Protein	T_m* (°C)	MutS binding			MutL binding
		K_d^{app} in FP# (nM)	K_d^{app} in SPR# (nM)	k_{off}^{app} in SPR# (s^{-1})	K_d^{app}in SPR# (nM)
WT MutS	43.2 ± 0.6	3.2 ± 0.5	69 ± 4	0.016 ± 2.7 *10^{-5}	15 ± 1
Aimed to promote stable coiled-coil					
STAB1	42.1 ± 0.9	0.95 ± 0.2	76 ± 6	0.027 ± 5.1 *10^{-5}	18 ± 2
STAB2	43.2 ± 0.7	2.5 ± 0.3	62 ± 9	0.018 ± 2.8 *10^{-5}	16 ± 2
STAB3	44.4 ± 1.0	2.5 ± 0.3	52 ± 11	0.009 ± 1.3 *10^{-5}	17 ± 2
STAB4	43.0 ± 0.5	1.2 ± 0.2	110 ± 23	0.009 ± 1.4 *10^{-5}	11 ± 2
Aimed to promote instable coiled-coil					
FLEX1	42.4 ± 1.0	22 ± 0.7	188 ± 17	0.029 ± 7.4 *10^{-5}	8.0 ± 1
FLEX2	41.7 ± 1.6	>670	978 ± 236	N/A	>1500
FLEX3	39.9 ± 0.8	>4600	N/A	N/A	N/A
Aimed to promote locked kink-out conformation					
LOCK1 – Crosslinked$	ND	ND	N/A	N/A	N/A
LOCK1$	38.6 ± 4.9	ND	28 ± 1	0.022 ± 3.8 *10^{-5}	N/A
WT$	ND	ND	30 ± 4	0.017 ± 2.4 *10^{-5}	
MIXED LOCK1$	ND	ND	93 ± 7.5	0.009 ± 1.2 *10^{-5}	N/A

*Standard deviation of three measurements are indicated after the ± sign.
#Standard errors of fitting are indicated after the ± sign.
$BSA was added to SPR running buffer at 1 mg/ml concentration.
N/A: parameters could not be determined, ND: experiment not performed.

DNA binding is affected by mutations in the kinking regions

To investigate whether the mutations in the coiled-coil influence DNA binding abilities, we used fluorescence polarization (FP) to measure equilibrium binding to a TAMRA-labeled DNA oligomer containing a GT mismatch (Table 2 and Figure 3). As predicted, all STAB-mutants showed comparable or stronger binding than WT. All FLEX-mutants that were designed to decrease the coiled-coil stability showed weaker DNA binding.

To investigate whether these differences in affinities for DNA originated from changes in binding kinetics, we performed SPR assays in which DNA binding kinetics can be assessed. The SPR measurements occur under flow conditions resulting in somewhat different affinity values compared to the FP measurements. However, the variations between mutants remained consistent between the two techniques. The STAB mutants show a similar K_d^{app}as WT except for STAB4. However, their apparent off rates are different (Table 2 and Figure 3C).

Destabilizing mutants, FLEX1, FLEX2 and FLEX3 all show faster dissociation rate, resulting into a weaker DNA affinity (Table 2 and Figure 3D). We also observed that mutating residues in helix 2 (FLEX2) have a larger effect on DNA affinity than mutating residues in helix 1 (FLEX1).

Analysis of sliding clamp formation and MutL recruitment

Next, we tested whether mutations in the coiled-coil of MutS would affect clamp formation and MutL loading on DNA (21). This analysis was not performed for MutS FLEX3 as it did not bind DNA sufficiently well for these assays. First, we analyzed ATP-induced release of blocked-end DNA as proxy for sliding clamp formation. We did this for all MutS STAB and FLEX mutants by performing SPR experiments with 100-bp heteroduplex DNA in the presence of ATP. All MutS mutants show slower dissociation on closed-end DNA than on open-end DNA (Supplementary Figure S2), indicating that all mutants are able to form the ATP-induced sliding clamp, which is required for MutL binding.

Next, MutL binding experiments were performed using the same oligo and ATP concentration as mentioned above, but now with titrations of MutL (Figure 3G). The binding response of the highest MutL concentration was plotted (Figure 3H) (individual experiments, Supplemental Figures S3 and S4).

We observed that WT, STAB1, STAB2, STAB3 and FLEX1 have a similar K_d^{app} for MutL binding (Supplementary Figure S4), showing that loading of MutL is not affected for these mutants. MutS FLEX2 has little MutL binding, likely due to poor DNA binding (Figure 3D). Finally, MutS STAB4 shows poor MutL binding on open heteroduplex DNA, compared to MutS WT, but it is not impaired on blocked DNA (Supplementary Figure S4).

As STAB4 binds mismatched DNA with an affinity in the same range as WT (respectively 110 ± 23 and 69 ± 4 nM), this could not explain the poor MutL recruitment on open DNA. We wondered if MutL binding itself was impaired, or whether the effect could be due to earlier steps.

To address this question, we further analyzed STAB4 behavior as a function of ATP. At a relatively high ATP concentration (32 μM), MutL stabilizes the WT protein on open-end DNA (Figure 4A). STAB4 is clearly impaired in this MutL-dependent stabilization, but we also noticed that STAB4 dissociates less than WT MutS (Figure 4A). Therefore, we analyzed dissociation from open-end DNA at different ATP concentrations (Figure 4B–E). We observed that STAB4 responds slower to ATP than WT (Figure 4B and C) indicating a defect in sliding clamp formation. Since sliding clamp formation and MutL binding are not impaired on blocked-end DNA, we can conclude that STAB4 may be

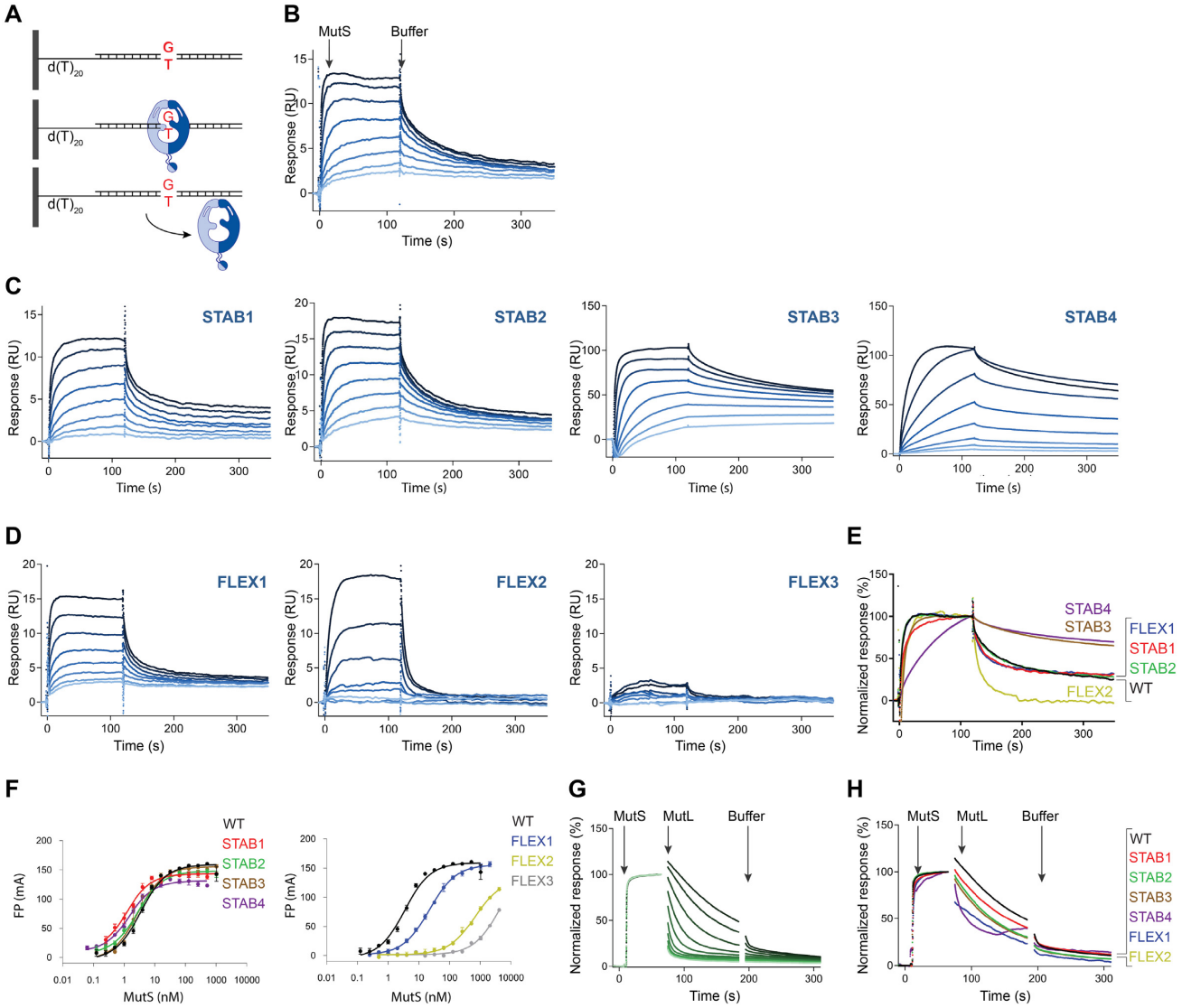

Figure 3. Binding of MutS mutants to mismatched DNA and MutL. (**A**) Schematic representation of SPR set-up. Biotinylated DNA consisting of 21 basepairs containing a GT mismatch and a Thymine-linker, immobilized on a streptavidin chip (top). MutS binds to the mismatch (middle) and will dissociate (bottom). (**B**) MutS WT binding curve with concentrations ranging from 5 to 640 nM. Starting with 120 s injection of MutS, followed by buffer injection for 240 s. (**C**) Binding curves for stabilizing mutants STAB1, STAB2, STAB3 and STAB4. (**D**) Binding curves for flexible mutants FLEX1, FLEX2 and FLEX3. (**E**) Binding curve of all MutS mutants and WT at 160 nM, normalized on maximum response at $t = 120$ s. (**F**) Equilibrium binding measurements using TAMRA-labeled 21-bp DNA containing a GT mismatch. Data points are averages between three measurements and error bars represent SEM. (**G**) Binding of MutS and MutL on 100-bp oligo, normalized on maximum MutS binding. MutL WT (concentrations ranging from 0 to 2048 nM) binding curve to MutS WT (1200 nM). The signal at $t = 65$–75 s and $t = 185$–195 s was removed due to the signal noise at the start and end of MutL injection. (**H**) Binding curves of MutL WT at concentration 2048 nM to all MutS constructs, normalized on maximum MutS binding (Supplementary Figures S4 and S5 for individual runs).

defective in the transition toward the MutL-activating state and that this affects MutL loading on open-end DNA.

Both monomers are able to kink-out and required for full DNA binding

In our crystal structure we observe two types of kink, one monomer kinking 'in' and one monomer kinking 'out'. We wondered whether this is a state that can bind DNA, or if this is only a conformation to 'open up' for DNA binding. To test this, we designed a mutant aimed to lock each monomer in the 'kinked-out' state by crosslinking of two cysteines irreversibly at either side of the hinge within the monomer. We introduced cysteines E435C and R449C into the cysteine free variant of MutS (19,20), creating MutS LOCK1 (Figure 2C). Addition of $BM(PEG)_3$ to LOCK1 generates the crosslink within the monomer. Binding abilities of LOCK1 and crosslinked LOCK1 to a 100-bp oligo were first verified via gel filtration analysis (Supplementary Figure S5). A peak shift, between 100GT50 and LOCK1–100GT50, shows binding of free LOCK1. However, this peak shift is absent when LOCK1 is crosslinked, indicating that crosslinked LOCK1 cannot bind 100GT50. To determine the kinetic parameters of LOCK1, with and without

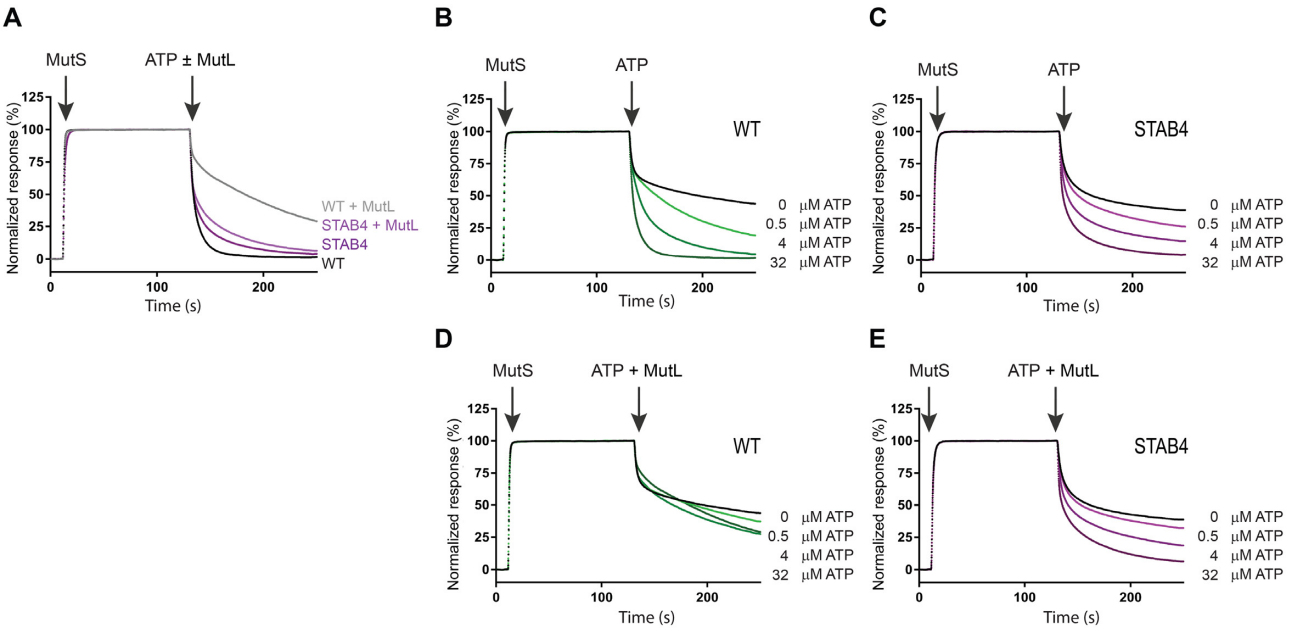

Figure 4. STAB4 is affected in ATP response and MutL binding. (**A**) MutS (1200 nM) was injected for 120 s in the absence of ATP on 100GT50, followed by a second injection containing either 32 μM ATP or 32 μM ATP + 400 nM MutL. MutS WT followed by ATP induced release (black) and bound by ATP and MutL (gray). MutS STAB4 with ATP (purple) and co-injected with MutL (pink). Binding is normalized on maximum MutS response. (**B**) MutS injection for 120 s (1200 nM), followed by 120-s injection of buffer (black) or 0.5, 4 or 32 μM ATP, respectively, in light to dark curves. (**C**) MutS STAB4 binding and dissociation, details see panel (B). (**D**) MutS injection for 120 s, followed by 120-s injection of buffer (black) or 0.5, 4 or 32 μM ATP supplemented with 400 nM MutL, respectively, in light to dark curves. (**E**) MutS STAB4 and MutL binding and dissociation, details see panel (D).

a crosslinker to heteroduplex DNA, SPR experiments were performed. These data showed that crosslinked LOCK1 has a poor DNA affinity (Figure 5B) too poor for further analysis. Unmodified LOCK1 shows DNA-binding kinetics similar to MutS WT (compare Figure 5A and B; Table 2).

To test the importance of both monomers in DNA binding, we generated heterodimers of unmodified and crosslinked LOCK1 by creating a mixed sample of unmodified LOCK1 and crosslinked LOCK1 in equimolar ratios to allow the heterodimers to form. We used 2-fold higher monomer concentrations, to account for an expected mixture of unmodified homodimer LOCK1, heterodimer and homodimer crosslinked LOCK1, distribution of 1:2:1. Although the actual distribution is unknown, the resulting mixture shows kinetic behavior of the mixture that is different from either of the homodimers (Figure 5C and B) indicating that heterodimers were produced and that the crosslinked coiled-coil affects the DNA -binding properties.

We conclude that kinking-movements are important in DNA loading since locked outward-kink LOCK1 shows very poor DNA binding and that heterodimers bind mismatched DNA with a weaker K_d^{app} but a slower k_{off} compared to non-crosslinked LOCK1 indicating that both monomers are important for DNA binding.

DISCUSSION

MutS is known to possess conformational freedom of its clamp domains in solution, as observed in SAXS studies (8) and in a previous crystal apo-structure of *Taq* MutS (11). However, the nature of this disorder remained unclear. In this work, we have tried to show that kinking of the helices in the lever domains of MutS can allow for movement of the clamp domains, as observed in the new apo-structure. Our measurements indicate that perturbation of the helical fold in these regions influences DNA-binding properties of MutS. Therefore, we hypothesize that kinking of coiled-coils as observed in this new crystal structure precedes DNA binding. Finally, crosslinked LOCK1 indicates that both monomers can kink outward and that they are both involved in full DNA binding.

Our structure is the first apo-structure for *E. coli* MutS. Recently, an apo-structure of MutS *Neisseria gonorrhoeae* was reported (29). The conformation of the clamp domains in ADP-bound MutS *N. gonorrhoeae* is rather different than in our structure. It has straight coiled-coils, without any kink in the lever domains, but with a somewhat more open conformation compared to mismatch-bound MutS.

All three MutS apo-structures are symmetrical in their nucleotide-state. DNA-free *Taq* MutS is lacking any nucleotide, our *E. coli* MutS structure has two ADP bound, as expected at this concentration of ADP (28,32). Both apo-structures of *N. gonorrhoeae* also have two nucleotides bound. *Neisseria gonorrhoeae* MutS has been crystallized in the presence of ADP (PDB: 5yk4). Surprisingly, on close inspection of the electron density maps, there is additional density visible, which could be explained by a third phosphate group. Possibly ATP or AMP-PNP were present, as in the second *N. gonorrhoeae* published structure (PDB: 5x9w) (29). It is possible that this nucleotide difference explains the differences in the lever domain conformation, relative to our ADP-bound kinked structure. Alternatively, the kinking is a stochastic process and the open form switches continually

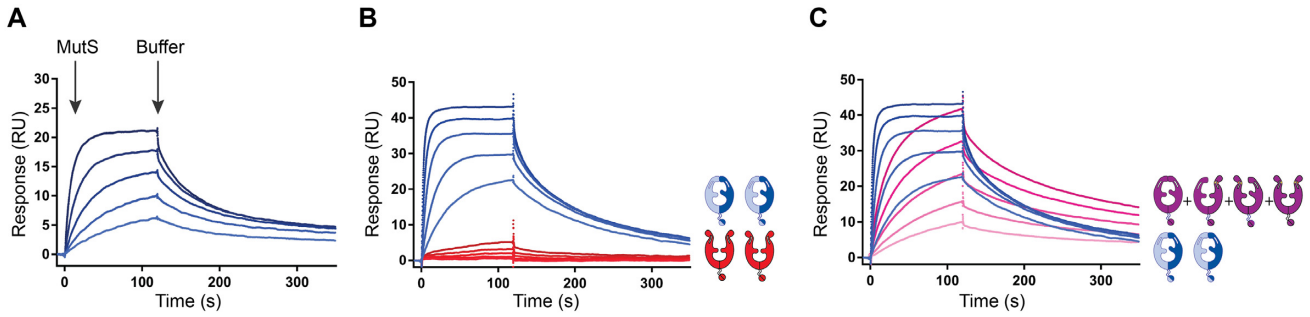

Figure 5. Stabilized kink (LOCK1) slows down kinetics of mismatched DNA binding. All SPR curves were performed in the presence of 1 mg/ml BSA. All runs started with 120-s injection of MutS, followed by buffer injection for 240 s. (**A**) SPR titration curve of MutS WT onto mismatched DNA with concentrations 5–80 nM. (**B**) SPR titration curve of MutS LOCK1 onto mismatched DNA with concentrations 8–128 nM. In blue MutS LOCK1, in red LOCK1 crosslinked with $BM(PEG)_3$. (**C**) Homodimer LOCK1 (see panel (B), blue) together with a 1:1 mixture of non-crosslinked and crosslinked (purple). Both constructs have a titration of 8–128 nM, making the total MutS concentration 16–256 nM.

between straight, kinked-in and kinked out states and the crystal traps a defined state.

Surprisingly, despite the difference in nucleotide state, all three apo-structures of MutS are lacking Mg^{2+} while it was present in each crystallization set-up. It may be explained by the fact that magnesium does not play a role in the equilibrium of ADP binding (32).

We made a series of mutants with the intention to analyze the importance of the defined kink for MutS function. Although we could not explicitly validate the structural impact of our mutations, they do affect DNA binding in opposing ways. Several mutants were designed to improve the stability of the coiled-coil (STAB3, 4), and these resulted in DNA binding with slower kinetics. This could indicate that 'opening' up of the dimer requires the ability to kink the helices. Conversely, the Pro/Gly/Pro motifs at the kinking sites in the FLEX-mutants were designed to destabilize the coiled-coil. These mutations had a very clear effect on DNA binding, where mutations in either of the two helices resulted in weaker binding to DNA, mainly due to faster release. In contrast to STAB3 and STAB4, the effect of Pro/Gly/Pro motif on DNA release is not balanced out by a comparable effect on association. Possibly, the effect on the helical stability is too big to form a stable MutS:DNA complex. The effect of introducing the Pro/Gly/Pro motif is less for residues 441–443 than for residues 515–517, inline with the smaller sequence change since residue 442 is already a glycine in the native protein.

We found that an intra-domain crosslink in the LOCK1 mutant severely affects DNA binding. This suggests that kinking of the lever domains is required for DNA binding. Since the dissociation rate of mixed LOCK1 is slower, it seems that both monomers need to be flexible for normal DNA binding and release.

All our mutants were able to form a sliding clamp on blocked DNA and able to recruit MutL. However, on open heteroduplex DNA, STAB4 did no longer bind MutL, although it still slides to some extent. This seems to be primarily caused by its weaker response to ATP, which may have slowed down the ability to arrive at the conformation required for MutL binding. Since it was still able to recruit MutL on closed-end DNA the slower sliding clamp formation may be the main defect in this mutant.

Our data suggest that the ability to rearrange the coiled-coil levers is important for MutS function. This is not necessarily a surprise, as flexibility of the coiled-coil-region was already shown to be important for related ABC-ATPases, such as the SMCs and RAD50 (15–18). What is surprising though, is that this flexibility appears as a sharp kink, rather than a gradual bend, although we believe that the precise kink angles may vary in the absence of crystal contacts. Sharp kinks have been observed in the coiled-coils of the SMC proteins by AFM and rotary shadowing EM (15,33). During revision of this manuscript, a paper appeared that revealed the presence of a defined kink in the structure of *E. coli* MukBEF and demonstrate its presence in *Saccharomyces cerevisiae* cohesin (34). The authors then show that discontinuity in the coiled-coils of related SMC proteins is a conserved feature in the SMC family suggesting that the so-called elbow movement is important for function. Together with our findings, this could open up a new mode of action for ABC-ATPase.

An interesting question is whether the hinge can respond by internal (e.g. ATP binding) or external (e.g. DNA binding) forces. Literature analysis does not give much precedent, with the exception of the 'buckling' observed in thermosensitive K(2P) channels coiled-coils and long α-helix filaments as a response to external stress to the ends of the helices (35,36). However, this type of force seems unlikely for MutS. Although it is theoretically possible that crystal contacts contributed to the kinked MutS state, our data indicate that the ability to move these regions may affect DNA binding. This suggests that the flexibility of the hinge region is used in the binding process. How this is organized will need further research.

In conclusion, we have found unexpected defined hinge points in the coiled-coil helices in the lever domains of MutS. It suggests a manner in which this protein can subtly achieve flexibility before adapting to the more ordered and probably favorable DNA-bound state. Some mutations in the hinging region have clear effects on DNA-Please check all figures are correctly placed and have no missing sections.binding properties of MutS, suggesting that there is a fine balance of the helical stability of the lever domains for proper DNA mismatch repair.

DATA AVAILABILITY

Access PDB code for the crystal structure is 6I5F.

SUPPLEMENTARY DATA

Supplementary Data are available at NAR Online.

ACKNOWLEDGEMENTS

We thank Robbie Joosten for critical analysis of the structure of MutS *N. gonorrhoeae* (PDB: 5yk4) and assistance in the refinement and Susanne Bruekner for her suggestion to lock MutS using a double cysteine mutant. Joyce Lebbink and Meindert Lamers provided useful comments on the manuscript.

Author Contributions: The crystal structure was solved and refined by A.F., with assistance from T.K.S. F.S.G., S.D. and D.B.K. performed mutant design and cloning. H.H.K.W., D.B.K. and S.D. performed purification of mutants. SPR experiments were performed by D.B.K. and A.F. Protein stability experiments were performed by A.F. FP experiments were performed by F.S.G. and S.D. Experiments regarding double cysteine mutants were performed by D.B.K. T.K.S. initiated and supervised the study and F.S.G. and D.B.K. wrote the manuscript with contributions of T.K.S. and A.F. and critical input from all authors.

FUNDING

Netherlands Organisation for Scientific Research (NWO) [714.016.002 (TOP), 711.011.011 (ECHO)]; CGC.nl as well as EU FP7 project [MM2M]. Funding for open access charge: Internal funds.

Conflict of interest statement. None declared.

REFERENCES

1. Kunkel,T.A. and Erie,D.A. (2005) DNA mismatch repair. *Annu. Rev. Biochem.*, **74**, 681–710.
2. Jiricny,J. (2013) Postreplicative mismatch repair. *Cold Spring Harbor Perspect. Biol.*, **5**, a012633.
3. Lynch,H.T. and de la Chapelle,A. (1999) Genetic susceptibility to non-polyposis colorectal cancer. *J. Med. Genet.*, **36**, 801–818.
4. Yamaguchi,M., Dao,V. and Modrich,P. (1998) MutS and MutL activate DNA helicase II in a mismatch-dependent manner. *J. Biol. Chem.*, **273**, 9197–9201.
5. Acharya,S., Foster,P.L., Brooks,P. and Fishel,R. (2003) The coordinated functions of the E. coli MutS and MutL proteins in mismatch repair. *Mol. Cell*, **12**, 233–246.
6. Calmann,M.A., Nowosielska,A. and Marinus,M.G. (2005) Separation of mutation avoidance and antirecombination functions in an Escherichia coli mutS mutant. *Nucleic Acids Res.*, **33**, 1193–1200.
7. Mendillo,M.L., Hargreaves,V.V., Jamison,J.W., Mo,A.O., Li,S., Putnam,C.D., Woods,V.L. Jr and Kolodner,R.D. (2009) A conserved MutS homolog connector domain interface interacts with MutL homologs. *Proc. Natl. Acad. Sci. U.S.A.*, **106**, 22223–22228.
8. Groothuizen,F.S., Fish,A., Petoukhov,M.V., Reumer,A., Manelyte,L., Winterwerp,H.H., Marinus,M.G., Lebbink,J.H., Svergun,D.I., Friedhoff,P. *et al.* (2013) Using stable MutS dimers and tetramers to quantitatively analyze DNA mismatch recognition and sliding clamp formation. *Nucleic Acids Res.*, **41**, 8166–8181.
9. Acharya,S., Wilson,T., Gradia,S., Kane,M.F., Guerrette,S., Marsischky,G.T., Kolodner,R. and Fishel,R. (1996) hMSH2 forms specific mispair-binding complexes with hMSH3 and hMSH6. *Proc. Natl. Acad. Sci. U.S.A.*, **93**, 13629–13634.
10. Lamers,M.H., Perrakis,A., Enzlin,J.H., Winterwerp,H.H., de Wind,N. and Sixma,T.K. (2000) The crystal structure of DNA mismatch repair protein MutS binding to a G x T mismatch. *Nature*, **407**, 711–717.
11. Obmolova,G., Ban,C., Hsieh,P. and Yang,W. (2000) Crystal structures of mismatch repair protein MutS and its complex with a substrate DNA. *Nature*, **407**, 703–710.
12. Warren,J.J., Pohlhaus,T.J., Changela,A., Iyer,R.R., Modrich,P.L. and Beese,L.S. (2007) Structure of the human MutSalpha DNA lesion recognition complex. *Mol. Cell*, **26**, 579–592.
13. Gupta,S., Gellert,M. and Yang,W. (2011) Mechanism of mismatch recognition revealed by human MutSbeta bound to unpaired DNA loops. *Nat. Struct. Mol. Biol.*, **19**, 72–78.
14. Lupas,A. (1996) Coiled coils: new structures and new functions. *Trends Biochem. Sci.*, **21**, 375–382.
15. Noort van,J., Heijden van der,T., Jager de,M., Wyman,C., Kanaar,R. and Dekker,C. (2003) The coiled-coil of the human Rad50 DNA repair protein contains specific segments of increased flexibility. *Proc. Natl. Acad. Sci. U.S.A.*, **100**, 7581–7586.
16. Eeftens,J.M., Katan,A.J., Kschonsak,M., Hassler,M., de Wilde,L., Dief,E.M., Haering,C.H. and Dekker,C. (2016) Condensin Smc2-Smc4 dimers are flexible and dynamic. *Cell Rep.*, **14**, 1813–1818.
17. Kamada,K., Su'etsugu,M., Takada,H., Miyata,M. and Hirano,T. (2017) Overall shapes of the SMC-ScpAB complex are determined by balance between constraint and relaxation of its structural parts. *Cell*, **25**, 603–616.
18. Kamada,K., Miyata,M. and Hirano,T. (2013) Molecular basis of SMC ATPase Activation: Role of internal structural changes of the regulatory subcomplex ScpAB. *Cell*, **21**, 581–594.
19. Manelyte,L., Urbanke,C., Giron-Monzon,L. and Friedhoff,P. (2006) Structural and functional analysis of the MutS C-terminal tetramerization domain. *Nucleic Acids Res.*, **34**, 5270–5279.
20. Winkler,I., Marx,A.D., Lariviere,D., Heinze,R.J., Cristovao,M., Reumer,A., Curth,U., Sixma,T.K. and Friedhoff,P. (2011) Chemical trapping of the dynamic MutS-MutL complex formed in DNA mismatch repair in Escherichia coli. *J. Biol. Chem.*, **286**, 17326–17337.
21. Groothuizen,F.S., Winkler,I., Cristovao,M., Fish,A., Winterwerp,H.H., Reumer,A., Marx,A.D., Hermans,N., Nicholls,R.A., Murshudov,G.N. *et al.* (2015) MutS/MutL crystal structure reveals that the MutS sliding clamp loads MutL onto DNA. *eLife*, **4**, e06744.
22. Battye,T.G., Kontogiannis,L., Johnson,O., Powell,H.R. and Leslie,A.G. (2011) iMOSFLM: a new graphical interface for diffraction-image processing with MOSFLM. *Acta Crystallogr. Sect. D Biol. Crystallogr.*, **67**, 271–281.
23. Evans,P. (2006) Scaling and assessment of data quality. *Acta Crystallogr. Sect. D Biol. Crystallogr.*, **62**, 72–82.
24. McCoy,A.J., Grosse-Kunstleve,R.W., Adams,P.D., Winn,M.D., Storoni,L.C. and Read,R.J. (2007) Phaser crystallographic software. *J. Appl. Crystallogr.*, **40**, 658–674.
25. Bricogne,G, B.E.,Brandl M, Flensburg,C, Keller,P, Paciorek,P, Roversi,P, Sharff,A, Smart,O, Vonrhein,C and Womack,T. (2010) *BUSTER Version 2.9*. Global Phasing Ltd, Cambridge.
26. Murshudov,G.N., Skubak,P., Lebedev,A.A., Pannu,N.S., Steiner,R.A., Nicholls,R.A., Winn,M.D., Long,F. and Vagin,A.A. (2011) REFMAC5 for the refinement of macromolecular crystal structures. *Acta Crystallogr. Sect. D Biol. Crystallogr.*, **67**, 355–367.
27. Joosten,R.P., Salzemann,J., Bloch,V., Stockinger,H., Berglund,A.C., Blanchet,C., Bongcam-Rudloff,E., Combet,C., Da Costa,A.L., Deleage,G. *et al.* (2009) PDB_REDO: automated re-refinement of X-ray structure models in the PDB. *J. Appl. Crystallogr.*, **42**, 376–384.
28. Monti,M.C., Cohen,S.X., Fish,A., Winterwerp,H.H., Barendregt,A., Friedhoff,P., Perrakis,A., Heck,A.J., Sixma,T.K., van den Heuvel,R.H. *et al.* (2011) Native mass spectrometry provides direct evidence for DNA mismatch-induced regulation of asymmetric nucleotide binding in mismatch repair protein MutS. *Nucleic Acids Res.*, **39**, 8052–8064.
29. Nirwal,S., Kulkarni,D.S., Sharma,A., Rao,D.N. and Nair,D.T. (2018) Mechanism of formation of a toroid around DNA by the mismatch sensor protein. *Nucleic Acids Res.*, **46**, 256–266.
30. Natrajan,G., Lamers,M.H., Enzlin,J.H., Winterwerp,H.H., Perrakis,A. and Sixma,T.K. (2003) Structures of Escherichia coli DNA mismatch repair enzyme MutS in complex with different

mismatches: a common recognition mode for diverse substrates. *Nucleic Acids Res.*, **31**, 4814–4821.
31. Arndt,K.M., Pelletier,J.N., Muller,K.M., Pluckthun,A. and Alber,T. (2002) Comparison of in vivo selection and rational design of heterodimeric coiled coils. *Structure*, **10**, 1235–1248.
32. Lebbink,J.H., Fish,A., Reumer,A., Natrajan,G., Winterwerp,H.H. and Sixma,T.K. (2010) Magnesium coordination controls the molecular switch function of DNA mismatch repair protein MutS. *J. Biol. Chem.*, **285**, 13131–13141.
33. Diebold-Durand,M., Lee,H., Ruiz Avila,L.B., Noh,H., Shin,H., Im,H., Bock,F.P., Burmann,F., Durand,A., Basfeld,A. *et al.* (2017) Structure of full-length SMC and rearrangements required for chromosome organization. *Cell*, **67**, 334–347.
34. Bürmann,F., Lee,B.-G., Than,T., Sinn,L., O'Reilly,F.J., Yatskevich,S., Rappsilber,J., Hu,B., Nasmyth,K. and Löwe,J. (2019) A folded conformation of MukBEF and cohesin. *Nat. Struct. Mol. Biol.*, **26**, 227–236.
35. Lolicato,M., Riegelhaupt,P.M., Arrigoni,C., Clark,K.A. and Minor,D.L. (2014) Transmembrane helix straightening and buckling underlies activation of mechanosensitive and thermosensitive K2P channels. *Neuron*, **84**, 1198–1212.
36. Palenčár,P. and Bleha,T. (2014) Buckling transition in long α-helices. *J. Chem. Phys.*, **141**, 174901–174912.